Overlapped Carrier-Sense Multiple Access (OCSMA) in Wireless Ad Hoc Networks

Surendra Boppana, *Student Member, IEEE,* and John M. Shea, *Member, IEEE*
(surendra@ufl.edu, jshea@ece.ufl.edu)

***Abstract*— In wireless ad hoc networks (WANets), multihop routing may result in a radio knowing the content of transmissions of nearby radios. This knowledge can be used to improve spatial reuse in the network, thereby enhancing network throughput. Consider two radios, Alice and Bob, that are neighbors in a WANet not employing spread-spectrum multiple access (SSMA). Suppose that Alice transmits a packet to Bob for which Bob is not the final destination. Later, Bob forwards that packet on to the destination. Any transmission by Bob not intended for Alice usually causes interference that prevents Alice from receiving a packet from any of her neighbors. However, if Bob is transmitting a packet that he had previously received from Alice, then Alice knows the content of the interfering packet, and this knowledge can allow Alice to receive a packet from one of her neighbors during Bob's transmission. In this paper, we develop a MAC protocol to support this technique in a WANet. We show how the 802.11 MAC protocol can be modified to allow for transmissions to be overlapped by taking advantage of noncausal knowledge of interfering signals. The resulting overlapped CSMA (OCSMA) protocol improves spatial reuse and end-to-end throughput in several scenarios.**

***Index Terms*— wireless ad hoc networks, MAC protocols, multi packet reception, interference cancellation.**

I. Introduction

Wireless networks present several challenging issues for the network designer that are quite different from their wired counterparts. An impairment that results due to the broadcast nature of the wireless network is interference. Since all the nodes share the same physical medium, simultaneous transmissions may result in interference at the receiving nodes. In networks that do not employ code-division multiple access, medium-access control (MAC) protocols are used to allocate the channel resources to specific transmitters and receivers so as to minimize the interference in the network. Traditionally, the design of the MAC protocol is carried out independently of the physical-layer design, assuming a simplistic collision channel model. These models assume the channel to be noiseless, and a packet is successfully received by a node if there are no other transmissions in its interference range. These MAC protocols schedule transmissions such that the collisions in the network are minimized.

Multi-user detection (MUD) in wireless networks has been proposed by several authors [1]–[7] as a means to increase spatial re-use by increasing the number of simultaneous transmissions in the network. MUD techniques are employed at the physical layer (PHY) to recover information from colliding packets at the receiver. These signal processing techniques used at the PHY enable a node to receive packets in the presence of other transmissions in its communication range. This multipacket reception (MPR) capability of the nodes at the physical layer leads to greater spatial re-use in the network. MAC protocols were proposed in [5], [8] that take advantage of the MPR capabilities of the physical layer to increase the spatial re-use in the networks to provide high-throughput in heavy traffic and low delay in light traffic.

However, in most cases, mobile radios might not have sufficient processing power to perform complex MUD schemes. The complexity of the MUD schemes could be significantly simplified and the performance enhanced if the interfering signal were completely known at the receiver. In wireless ad hoc networks, the interfering signal may be known at the receiver due to multihop routing. For example, consider a four-node linear network consisting of nodes A, B, C and D, where A transmits a packet to D using multihop routing. In a slotted communication system employing conventional MAC protocol, a typical sequence of transmissions for a packet would be

$$1 : \mathrm{A} \rightarrow \mathrm{B},\ 2 : \mathrm{B} \rightarrow \mathrm{C},\ 3 : \mathrm{C} \rightarrow \mathrm{D},$$

where the notation $1 : \mathrm{A} \rightarrow \mathrm{B}$ indicates that node A transmits a packet to node B in time slot 1, etc. Under conventional MAC protocols, in the time slot when C forwards a packet to D, A is not allowed to transmit to B since C's transmission will cause interference at B. However when a MPR-based MAC protocol is employed, simultaneous transmissions of A→B and C→D are possible, since MUD techniques can be employed at B to recover the packet transmitted by A. Note that the packet transmitted by C to D is the same packet that B forwarded to C in an earlier time slot (ignoring the differences in the headers). If B were to retain a copy of the packet that it forwarded to C, B would have information regarding the interfering transmission. This greatly reduces the complexity of the MUD algorithms employed at the PHY to recover the packet transmitted by A. This example is revisited in Section II.

The idea of employing known-interference cancellation (IC) techniques to increase simultaneous transmissions in ad hoc networks was first analyzed in [9]. In our previous work, knowledge of the interfering signal is assumed at both the transmitter and the receiver, and the receiver performs MUD/IC to recover additional messages. Limitations on scheduling such simultaneous transmissions were analyzed and a MAC protocol that supports such simultaneous transmissions was proposed.

The idea of employing network coding to increase spatial re-use and throughput in wireless ad hoc networks has recently received considerable attention from the research community [10]–[16]. A

The material in this paper was presented in part at Military Comm. Conf. Oct. 2007, Orlando FL.

This work was supported by the National Science Foundation under grant number CNS-0626863, and by the Air Force Office of Scientific Research under grant number FA9550-07-10456.

transmitting node exploits the broadcast nature of the physical medium along with the knowledge of the interfering messages at the receiving nodes to combine/encode multiple independent messages at the network layer and transmit to several nodes. A node receiving the encoded message, uses the knowledge of the other interfering messages, available at the network layer, to recover the message intended for it. Practical channel sharing schemes that support network coding in wireless ad hoc networks were proposed in [11], [13], [15]. The idea of employing network coding at the physical layer to increase simultaneous transmissions in wireless ad hoc networks was considered in [17]–[20]. A node receiving a signal consisting of several simultaneous transmissions employes the knowledge of the interfering signals, available at the physical layer, to recover the message intended for it. This approach is similar to the idea of employing MUD with known-interference cancellation. These works analyze the physical-layer aspects involved, but do not address the MAC-layer implications of employing such simultaneous transmission schemes. In this work, we analyze some of the fundamental limits involved in employing MUD/IC based techniques to accommodate simultaneous transmissions in the network. Our analysis provides an understanding of the performance gains of such transmissions, and an insight into the PHY and MAC interaction required for scheduling such transmissions. We also design a MAC protocol based on the IEEE 802.11 MAC protocol which exploits this feature to improve the spatial re-use and throughput in wireless networks.

The rest of the paper is organized as follows. Section II introduces the idea of employing overlapped transmission in a linear network. In Section III, some limits on performing overlapped transmissions in wireless networks are evaluated. Section IV describes the OCSMA MAC protocol. The design issues of the protocol are considered in Section V, and Section VI provides performance evaluation of the protocol. The paper is concluded in Section VII.

II. Motivation

In this section, we illustrate the idea of overlapped transmissions in a four-node linear network, which is illustrated in Fig. 1. We assume that the nodes can communicate only with the adjacent nodes and operate in the half-duplex mode. Node A transmits packets to node D through multihop routing. A typical transmission sequence under a conventional scheduling scheme is depicted in Fig. 1, in which it takes three time slots for a packet from A to reach D. The scheduled transmissions in a given time slot are marked by solid directed arrows along with the packet identifiers, and the interference caused by these transmissions are marked by dashed arrows. Under typical carrier-sense multiple access protocols with collision avoidance (CSMA/CA), when packet m_1 is being forwarded by C in time slot t_3, A cannot transmit the message m_2 since C's transmission will cause interference at B.

The throughput of this network can be improved by employing simultaneous transmissions as described below. We observe that in the time slot t_3, C forwards the packet m_1 which it received from B in the earlier time slot t_2. If B were to retain a copy of the message m_1 locally, it knows the message being transmitted by C in time slot t_3 (assuming that link-level encryption is not used and any differences in the headers are ignored). If A is allowed to transmit the message m_2 in the time slot t_3, B can use the stored

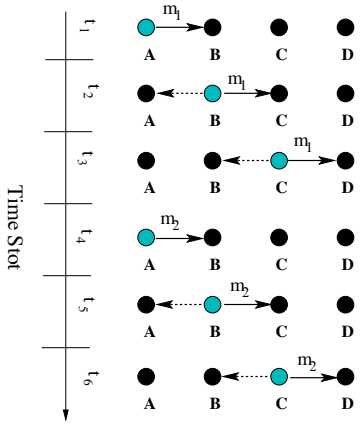

Fig. 1. Four-node linear network with conventional scheduling.

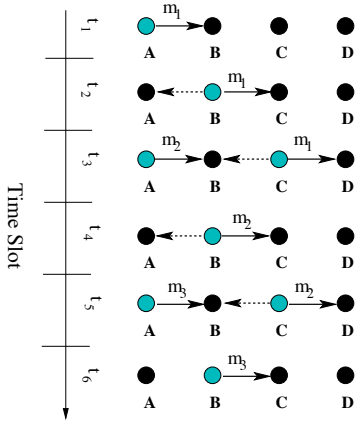

Fig. 2. Four-node linear network with overlapped transmissions.

information regarding m_1 to mitigate the interference caused by C's transmission. We call this additional transmission that results due to the interference mitigation of known interference as *overlapped transmission*.

A scheduling scheme employing the idea of overlapped transmission for the four-node linear network is depicted in Fig. 2. Under this scheduling scheme, a packet is transmitted from A to B employing overlapped transmission strategy during the time slot that C forwards a packet to D. Since the transmission of the packet from A to B did not involve the allocation of a separate time slot for its transmission, a packet requires on an average only two time slots to be transmitted from A to D. These two time slots are required for the scheduling of transmissions from B to C, and C to D, respectively. The performance gain of this scheduling scheme can be measured in terms of transmission efficiency, which is defined as the ratio of the time taken for the transmission of M packets under conventional scheduling scheme and the scheduling scheme employing overlapped transmissions, respectively. The transmission efficiency Γ_4 of this scheme is given by

$$\Gamma_4 = \frac{3M}{2(M-1)+3}, \quad \approx \frac{3}{2}, \ M \gg 1, \tag{1}$$

where M is the total number of packets transmitted by A. Note that under conventional scheduling, it takes three time slots for

every packet from A to reach D. However, using the scheduling scheme employing overlapped transmissions, it takes two time slots on average for a packet from A to reach D [1].

Similarly, in an $N(N \geq 4)$ node linear network, the transmission efficiency Γ_N, of the scheduling scheme employing overlapped transmissions can be shown to be

$$\Gamma_N = \frac{N-1+3(M-1)}{N-1+2(M-1)}, \quad \approx \frac{3}{2}, \ M \gg 1. \tag{2}$$

We observe that the centralized scheduling scheme employing overlapped transmissions has the potential to improve the efficiency of a linear network by up to approximately 50% over the conventional scheme. In Section III, we look at some of the limitations of employing overlapped transmissions in ad hoc networks, and in Section IV we develop a MAC protocol that supports overlapped transmissions in wireless networks. Since the focus of this work is on developing a MAC protocol that supports overlapped transmissions, the physical layer aspects of the protocol are not evaluated here.

We identify a transmission between two nodes as a *primary transmission* if the transmission is not predicated on the use of non-causal knowledge of the interfering signals during that transmission interval. For example, in the network of Fig. 2, the transmission of message m_1 from C to D in time slot t_3 is the *primary transmission*, and the nodes C and D are called the *primary transmitter* and the *primary receiver*, respectively. Similarly, a transmission between two nodes is a *secondary transmission* if at least one of the nodes has non-causal information about the primary transmissions in the present transmission interval and performs MUD/IC to mitigate the interference. In the network of Fig. 2, the transmission of the message m_2 from node A to B in time slot t_3 for which B performs MUD/IC to mitigate the interference from C's transmission is the *secondary transmission* and the nodes A and B are called the *secondary transmitter* and *secondary receiver* respectively.

III. Overlapped Transmission in Wireless Ad Hoc Networks

A. System Model

Consider first a wireless ad hoc network with nodes distributed according to a two-dimensional Poisson point process with density λ nodes per unit area. Each node is equipped with a transceiver and communicates with other nodes in half-duplex mode. We assume that each node has an infinite packet buffer, and each radio retains copies of the packets it forwards unless that packet is transmitted to its final destination or until that packet has been forwarded on by one of its neighbors. To investigate some of the issues that will limit the performance of overlapped transmission, we analyze the use of overlapped transmission in a system using slotted communications. In this model, each node transmits in a given time slot with probability p. This assumption is only to facilitate the analysis of overlapped transmissions in ad hoc networks in Section III. However, no such assumption is made during the development of the MAC protocol in Section IV, or the network simulations in Section VI. We also assume that the secondary transmitter is informed of the corresponding primary transmission, and the overlapped transmission is synchronized with its corresponding primary transmission. The received power P_r can be expressed as

$$P_r = K_p d_r^{-\alpha} P_t, \tag{3}$$

where P_t is the transmitted power, d_r is the distance between the transmitter and the receiver, K_p is a constant, and α is the path-loss exponent. In the absence of interference, we assume that a transmission at the maximum power level will be received correctly if and only if the intended receiver is within a distance of one unit from the transmitter. The interference range is assumed to be twice the transmission range. Nodes within the interference range but outside the transmission range of a transmitter can detect the presence of a transmission but will not be able to correctly decode the packet being transmitted. In this section,

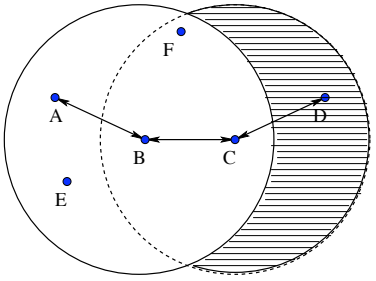

Fig. 3. Ad hoc network.

we consider some limitations on the ability to utilize overlapped transmissions to improve the throughput in a wireless ad hoc network. These limitations come from the following two sources:

- *Interference due to secondary transmission:* Since the secondary receiver has non-causal knowledge of the primary transmission, it can mitigate the interference due to the primary transmitter and recover the intended message. However, the secondary transmission causes interference, possibly to several primary transmissions. In Section III-B, we evaluate the amount of interference that the secondary transmission causes at the primary receiver, and how this interference can be controlled by adapting the power level of the secondary transmission to meet specified signal-to-interference ratio (SIR) and outage requirements.
- *Probability of secondary transmission:* Overlapped transmissions depend on the availability of suitable secondary transmitters and the successful reception of the messages at the secondary receiver.

The analytical results in Sections III-B and III-C are based on the network shown in Fig. 3, which can be considered to be a part of a larger network. Nodes A and C are two nodes in the transmission range of B, and B transmits packets to D through C by employing multihop routing. Hence D is in the transmission range of C, but not in the transmission range of B. This particular region is shown in Fig. 3 with dashed lines. We also assume that A has packets for B. The network of Fig. 3 is used to simplify the analysis, yet illustrate the important aspects of overlapped transmission.

B. Interference due to secondary transmission

Consider first the ad hoc network of Fig. 3, and the time slot during which node C forwards to D a packet which it has received

[1]The first packet requires three time slots.

from B in an earlier transmission. The transmission from C to D is a primary transmission, and a possible secondary transmission would be node A transmitting a packet to node B. We assume that both nodes A and B are informed of C's transmission to D. Node A is allowed to transmit only if it is not in the transmission range of D. This restriction on A's transmission reduces the amount of interference at D, but it is still non-negligible. Note that as stated in the Section III-A, we assume that the interference range is twice the transmission range. However, A is allowed to transmit even if it is in the transmission range of C. We also assume that B can perform perfect interference cancelation of C's transmission and recover the packet transmitted by A. However, A's transmission causes interference at node D. In order to analyze the impact of the secondary transmission at the primary receiver, we evaluate the Signal-to-Interference Ratio (SIR) at node D. We assume that the secondary transmission is the only source of interference at D.

For conciseness, we introduce the following notation. Let X_{ij} be the random variable denoting the distance between the nodes i and j. Also, let $\mathcal{A}_l(r_1, r_2, d)$ denote the area of the lens formed by the intersection of two circles of radii r_1 and r_2 with centers separated by a distance d. Mathematically,

$$\begin{aligned}\mathcal{A}_l(r_1,r_2,d) \;=\; & r_1^2\cos^{-1}\left(\frac{r_1^2+d^2-r_2^2}{2r_1d}\right)\\ & + r_2^2\cos^{-1}\left(\frac{r_2^2+d^2-r_1^2}{2r_2d}\right)\\ & -0.5\left[\sqrt{(r_1+r_2+d)(r_1+r_2-d)}\right.\\ & \times\left.\sqrt{(r_1-r_2+d)(-r_1+r_2+d)}\right]. \quad (4)\end{aligned}$$

Let ρ denote the ratio of the distances between nodes C and D, and A and D respectively. Mathematically,

$$\rho = \frac{X_{CD}}{X_{AD}},\ X_{CD}<1,\ X_{AD}>1. \quad (5)$$

The constraint $X_{CD} < 1$ indicates that D is in the transmission range of C and the constraint $X_{AD} > 1$ reflects the fact that the secondary transmitter A is allowed to transmit only if it is not in the transmission range of D. Hence we have $\rho < 1$. In an exponential path-loss channel without fading, the ratio γ of the powers of the primary transmission to the secondary transmission at node D can be expressed as

$$\gamma = \left(\frac{X_{CD}}{X_{AD}}\right)^{-\alpha} = \rho^{-\alpha},\ \rho<1. \quad (6)$$

The density of ρ can be expressed as

$$f_\rho(r) = \int_{s>1} s f_{X_{AD},X_{CD}}(s, rs)ds, \quad (7)$$

where $f_{X_{AD},X_{CD}}(s,y)$ is the joint probability density function (pdf) of X_{AD} and X_{CD}. The joint pdf of X_{AD} and X_{CD} is evaluated in Appendix I and is given by (19). The truncated distribution of ρ is given by

$$f_\rho(r|r<1) = \begin{cases}\frac{f_\rho(r)}{\int_0^1 f_\rho(r)dr}, & 0\le\rho<1,\\ 0, & \text{otherwise.}\end{cases} \quad (8)$$

The pdf of the SINR γ, can be obtained from the pdf of ρ using the transformation

$$f_\Gamma(\gamma) = \frac{1}{\alpha}\gamma^{-1-\frac{1}{\alpha}} f_\rho(\gamma^{-\frac{1}{\alpha}}|\gamma^{-\frac{1}{\alpha}}<1), \quad (9)$$

where α is the path-loss exponent. The distribution function

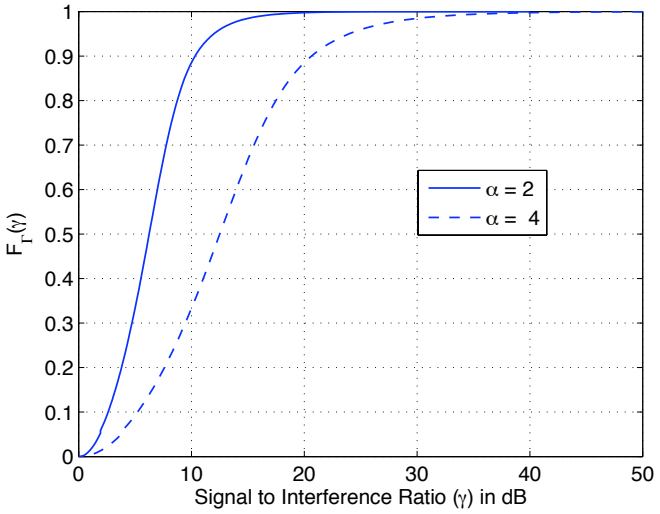

Fig. 4. Distribution of signal-to-interference ratio, γ.

$F_\Gamma(\gamma)$ of the SIR γ at D for path-loss exponents $\alpha = 2, 4$ are numerically computed and plotted in Fig. 4. Let γ_0 denote the minimum SIR requirement for the successful reception of a message at a radio. An outage event occurs when the SIR γ, falls below γ_0. Let β denote the the outage probability,

$$\Pr(\gamma \le \gamma_0) < \beta. \quad (10)$$

Since the radio locations are random, it may not possible to achieve $\beta = 0$ for a particular γ_0. For example, let $\alpha = 4$, $\beta = 0.05$ and $\gamma_0 = 12$ dB. This SIR requirement roughly translates to the secondary transmitter being at a distance of two units from the secondary receiver. From Fig. 4, we have for $\beta = 0.05$, SIR of $F_\Gamma^{-1}(\beta) = 4$ dB which is less than the required SIR. The interference caused by the secondary transmission can be controlled by using the location information of the nodes in choosing the secondary transmitter. Another way to meet the target SIR requirement without increasing the interference to other nodes is to reduce the power of the secondary transmission.

C. Probability of secondary transmission

In this section, we evaluate the probability of a secondary transmission given that there is a primary transmission which permits a secondary transmission. With respect to the network of Fig. 3, given that C successfully forwards B's packet to D, we evaluate the probability of a successful secondary transmission from node A to B. The probability of a successful secondary transmission depends on the following factors.

1) Availability of a secondary transmitter (arbitrarily called node A here): All the nodes that are in the transmission range of secondary receiver (node B), but not in the transmission range of the primary receiver (node D) are identified as potential secondary transmitters. One of them is arbitrarily chosen as the the secondary transmitter. We

note that identification of a secondary transmitter does not guarantee a successful secondary transmission. In this analysis, we do not address the issue of how a secondary transmitter is chosen, but investigate the factors that limit the availability of a secondary transmitter.

2) Availability of packets at the secondary receiver: In order to simplify the analysis, we assume that a secondary transmitter always has packets for the corresponding receiver.
3) Scheduling a secondary transmission: We assume that, once a secondary transmitter is identified, it transmits a packet to the secondary receiver, independent of the state of the medium. This secondary transmission may cause interference to several primary transmissions, however, as discussed in Section III-B, the interference can be reduced to an acceptable level by reducing the power of the secondary transmission. This assumption results in an upper bound on the probability of scheduling a secondary transmission in a time slot.
4) Successful reception of the overlapped data at the secondary receiver: The secondary receiver can successfully receive the message, provided that no node in its interference range, with the exception of the primary transmitter, about which it has information, transmits. We do not consider the effect of other secondary transmissions at this secondary receiver as this interference can be minimized by reducing the transmission power. This provides an upper bound on the number of overlapped transmissions that can occur in an ad hoc network.

With respect to the example network of Fig. 3, we evaluate the probability of a successful secondary transmission from node A to B while C successfully forwards to D the packet it has received from B in an earlier transmission. Based on the above discussion, the probability of a successful secondary transmission, $\mathrm{p}(\mathcal{S})$ can be mathematically represented as

$$\mathrm{p}(\mathcal{S}) \leq \mathrm{p}(\mathcal{F})\mathrm{p}(\mathcal{T}|\mathcal{F}), \tag{11}$$

where $\mathcal{F}$ denotes the event that there is a suitable secondary transmitter (denoted as A in our example network), and $\mathcal{T}$ denotes the event that the secondary receiver (denoted as B in our example network) successfully receives the packet transmitted by the secondary transmitter.

The probability of the event $\mathcal{F}$ is equivalent to finding a non-transmitting node which is in the transmission range of B, but not in the transmission range of D. This region $A_F(z)$ is given by

$$A_F(z) = \mathcal{A}_l(1, 1, z), \ 1 < z \leq 2, \tag{12}$$

where $\mathcal{A}_l(r_1, r_2, d)$ is given by (4) and z is the distance between B and D whose pdf is given by

$$f_{X_{BD}}(z) = \int_x \int_y f_{X_{CD},X_{BD}}(y, z|X_{BC} = x) f_{X_{BC}}(x) dy dx, \tag{13}$$

where $f_{X_{CD},X_{BD}}(y, z|X_{BC} = x)$ and $f_{X_{BC}}(x)$ are given by (18) and (16), respectively. Since the nodes are Poisson distributed with node density λ, the probability $\mathrm{p}(\mathcal{F})$, of finding a secondary transmitter is given by

$$\begin{aligned} \mathrm{p}(\mathcal{F}) &= \int_z \sum_{n=0}^{\infty} \frac{(\lambda \mathcal{A}_F(z))^n e^{-\lambda \mathcal{A}_F(z)}}{n!} (1 - p^n) dz \\ &= 1 - \int_z e^{-\lambda \mathcal{A}_F(z)(1-p)} f_{X_{BD}}(z) dz, \end{aligned} \tag{14}$$

where p is the probability of transmission by a node in a time slot. The probability $\mathrm{p}(\mathcal{F})$, of finding a secondary transmitter is shown in Fig. 5 for three different node densities, λ. It can be seen that for a given probability of transmission in a time slot, the probability of finding a secondary receiver increases with an increase in the node density. Also note that for stable operation of the network, the probability of transmission p, should be less than the average number of nodes in the interference range of a node. In our system, this corresponds to $p \leq (4\pi\lambda)^{-1}$, where λ is the node density, and the interference range of a node is assumed to be 2 units. With $p = (4\pi\lambda)^{-1}$, $\mathrm{p}(\mathcal{F})$ is 0.51, 0.74 and 0.85 for $\lambda = 1, 2,$ and 3, respectively. The probability $\mathrm{p}(\mathcal{T}|\mathcal{F})$,

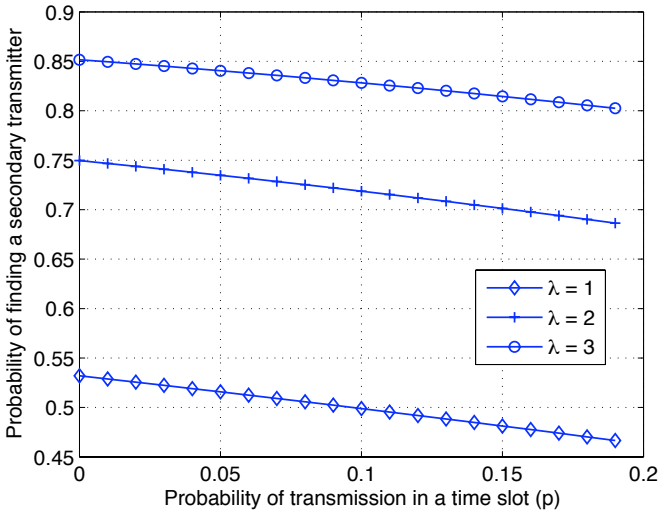

Fig. 5. Probability of finding a secondary transmitter.

of successful reception of a secondary transmission is equivalent to B receiving a packet from A. B can successfully receive a packet from A if no node in the non-overlapping interference regions of B and D transmits. As noted earlier, the effect of only the primary transmissions are taken into consideration. This assumption provides an upper bound on the number of overlapped transmissions possible. This region $\mathcal{A}_I(z)$ is given by

$$\mathcal{A}_I(z) = \mathcal{A}_l(2, 2, z) \tag{15}$$

where $\mathcal{A}_l(r_1, r_2, d)$ is given by (4). The probability $p(\mathcal{T}|\mathcal{F})$ that B successfully receives a packet from A is given by

$$\begin{aligned} p(\mathcal{T}|\mathcal{F}) &= \int_z \sum_{n=0}^{\infty} \frac{(\lambda \mathcal{A}_I(z))^n e^{-\lambda \mathcal{A}_I(z)}}{n!} (1 - p)^n dz \\ &= \int_z e^{-\lambda \mathcal{A}_I(z) p} f_{X_{BD}}(z) dz, \end{aligned}$$

where p is the probability of transmission of a node in a time slot, and $f_{X_{BD}}(z)$ is the pdf of X_{BD} given by (13). The probability

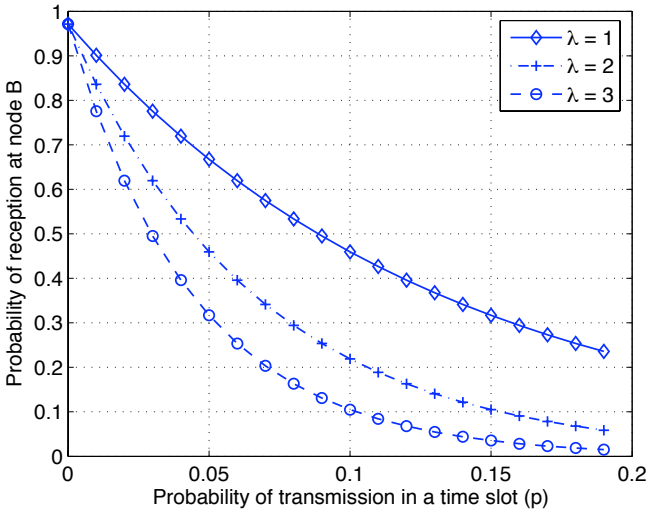

Fig. 6. Probability of reception by node B.

of reception by node B was numerically evaluated and the pdf is plotted in Fig. 6 for three different node densities, λ. The path-loss exponent, $\alpha = 4$. As the node density increases, the probability of reception decreases, which is due to the increase in the interference around node B. For an ad hoc network with probability of transmission $p = (4\pi\lambda)^{-1}$, the probability of node B receiving A's message is 0.53 for all the node densities λ. The upper bound on the probability of successful secondary

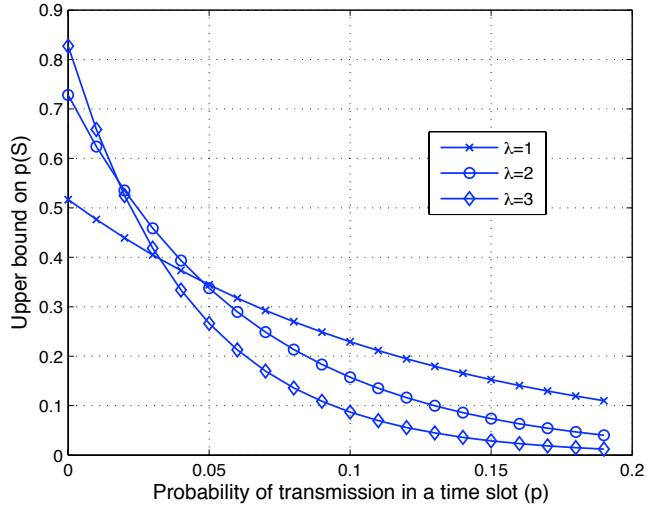

Fig. 7. Upper bound on the probability of a successful secondary transmission, $p(\mathcal{S})$.

transmission $p(\mathcal{S})$ (refer to (11)) is shown in Fig. 7 for several values of node densiy λ. When the probability of transmission, $p = (4\pi\lambda)^{-1}$, the value of the upper bound is 0.27, 0.39, and 0.41 for $\lambda = 1, 2,$ and 3, respectively. For $p = (8\pi\lambda)^{-1}$, the value of the upper bound is 0.37, 0.54, and 0.61 or $\lambda = 1, 2,$ and 3, respectively.

The preceding analysis shows that there is a high probability of successful secondary transmission given that there is primary transmission in the given time slot. Although this secondary transmission causes interference to several primary transmissions, this interference can be minimized by either selecting secondary transmissions that are outside of the primary receiver's interference range, or by reducing the power of the secondary transmission. Simplifications on the system model were made in order to gain insight into the factors governing overlapped transmissions in an ad hoc network. In the following sections we develop a MAC protocol which supports overlapped transmissions in wireless networks, and evaluate its performance under various network scenarios.

IV. Overlapped Carrier Sense Multiple Access (OCSMA) Protocol

The OCSMA protocol is based on the distributed coordinated function (DCF) mode of the IEEE 802.11 MAC protocol [21]. Unless stated explicitly, the terminology used in the following sections reflects the MAC protocol description of the IEEE 802.11 standard.

The design of the OCSMA protocol is best described with the example network of Fig. 8(a). The timeline of the protocol for the example network is shown in Fig. 9, and the frame formats are shown in Fig. 10. The operation of the protocol can be divided into five phases as follows:

A. Primary Handshaking

This phase of the OCSMA protocol is similar to the RTS/CTS exchange of the IEEE 802.11 protocol. When a node has data to transmit to another node in its transmission range, it initiates the handshake by sending a Request To Send (RTS) frame. The node that receives the RTS sends a Clear To Send (CTS) frame if it senses the medium to be free. The node initiating the handshake is the *primary transmitter* and the node that responds to the RTS is the *primary receiver*. All the other nodes that receive the handshake set their transmit allocation vectors (TAV) for the duration of the transmission. The transmit allocation vector is similar to the network allocation vector (NAV) defined in the IEEE 802.11 standard. However, as described below there are some significant differences between them.

The MAC of each receiver is equipped with a transmit allocation matrix (TAX) which is responsible for the virtual carrier sense mechanism. The TAX is an array of several transmit allocation vectors (TAV). Nodes receiving a valid frame that is not destined for them update their TAV with the information in the Duration/ID field. Unlike the NAV vector of IEEE 802.11, the TAX allocates a TAV for each valid frame (not addressed to the receiving node) it receives, even if the new TAV value is not greater than any of the current TAVs. Thus the TAX maintains an array of TAVs for each frame that it receives. The medium is considered busy if any of the TAVs is set. The TAVs also store information regarding the transmitter and receiver of the frame, if that information is available. The implementation of the TAX greatly simplifies the design of OCSMA protocol, as discussed in later sections. Another important distinction between NAV and TAV is that a node can transmit even if the TAV of a node is set. The conditions under which this is possible are discussed later.

Consider the wireless ad hoc network shown in Fig. 8(a), where at some point of time, node C intends to forward a packet to D that it has received from B in an earlier transmission. C transmits an RTS to D, and D responds with a CTS. The primary handshaking phase is depicted in Figs. 8(b) and 8(c).

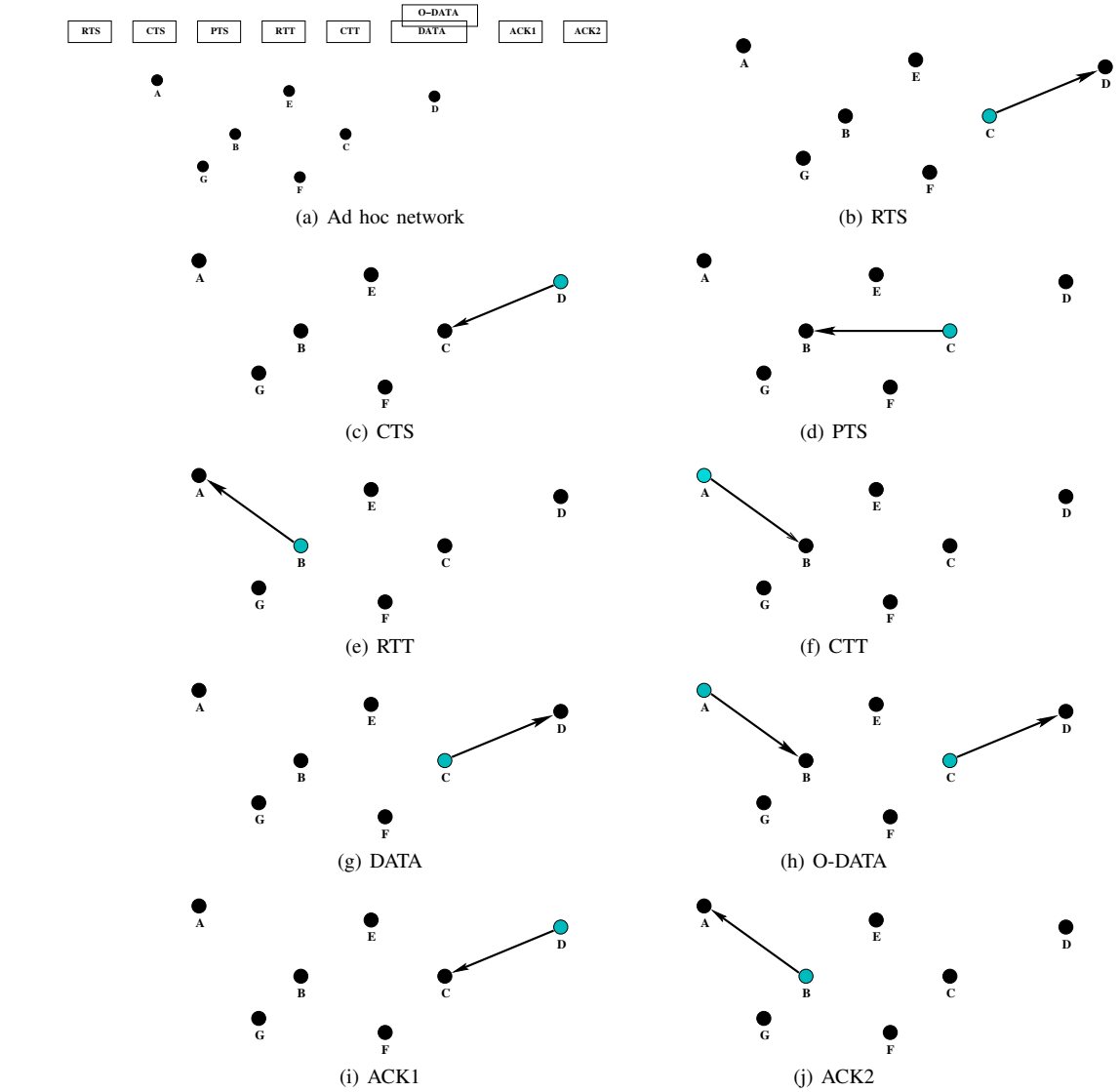

Fig. 8. Typical frame exchanges in OCSMA protocol.

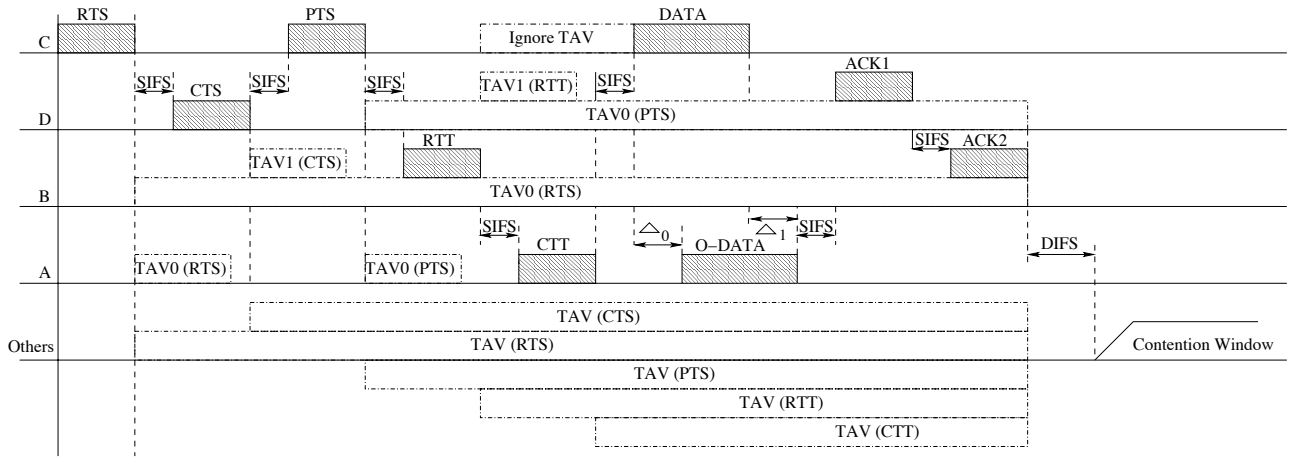

Fig. 9. Timeline of the OCSMA protocol.

B. Secondary Handshaking

The secondary handshaking can be thought of as a secondary RTS/CTS exchange employed to determine the possibility of an overlapped transmission during the present transmission interval. Upon receipt of the CTS, the primary transmitter sends a Prepare

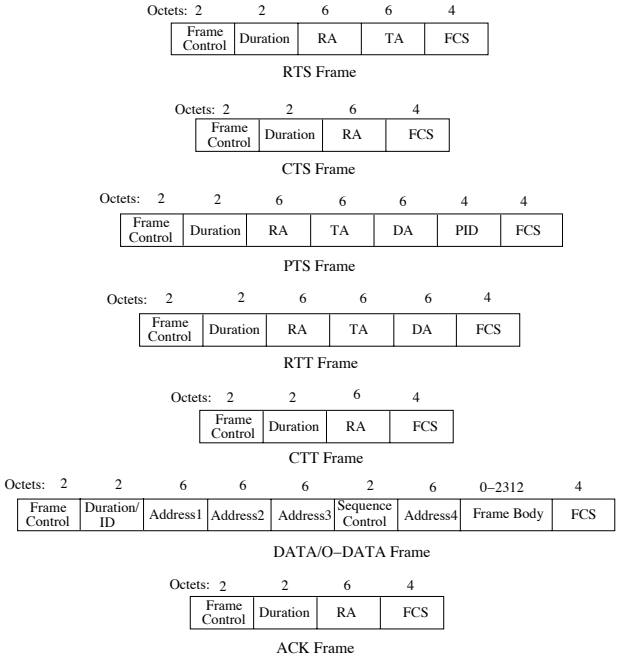

Fig. 10. Frame formats of the OCSMA protocol.

To Send (PTS) frame to the node from which it received this particular data frame in an earlier transmission. If the data is locally generated, no PTS is sent and transmission of the data frame starts after SIFS, as in the 802.11 protocol [21]. If the PTS is sent, the primary transmitter defers transmission of the data frame until the completion of the secondary handshaking. The TAX ensures that none of the TAVs of the primary transmitter are set by the control frames corresponding to the secondary handshaking initiated by this node.

In the network of Fig. 8(a), consider a transmission in which node C forwards to D a data frame that it previously received from B. After the completion of RTS/CTS exchange with D, C sends a PTS to B.

The PTS frame format is shown in Fig. 10. The format is similar to the format of an RTS frame except for the additional fields DA and PID. DA contains the address of the primary receiver and PID contains the unique ID of the data frame that is being transmitted to the primary receiver. The node receiving the PTS frame is called the *secondary receiver*. Being a secondary receiver implies that the present node has information regarding the primary transmission and is capable of receiving an overlapped transmission.

Upon receipt of the PTS, the secondary receiver ensures that its TAV is set only by the primary transmitter. Note that the TAVs store information regarding the transmitter and receiver of any valid frame it receives that is not addressed to the receiving node. This is to ensure that there are no other transmissions occurring in the range of the secondary transmitter except for the primary transmission. If this is true, it identifies a suitable partner for secondary transmission as described below.

Once the secondary receiver identifies the medium to be free except for the primary transmission, it generates a list of potential partners. The nodes are identified based on the following criteria:

1) The node should not be in the transmission range of the primary receiver.
2) The node should have transmitted a frame to the secondary receiver in an earlier time slot. The information regarding receipt of frames from all the other nodes is maintained in a cache at the MAC level.

The second condition is based on the heuristic that if a node has transmitted a frame to the secondary receiver in an earlier time slot, it is very likely that there might be more frames destined for the secondary receiver. This ensures that there is a greater probability of secondary transmission for any particular partner. A node is chosen randomly[2] from the potential candidates to be the *secondary transmitter*.

Once the secondary transmitter is identified, the secondary receiver sends a Request to Transmit (RTT) frame to the secondary transmitter. The format of RTT is similar to the format of RTS except that it also contains additional information regarding the address of the primary transmitter (DA field). The secondary transmitter compares the address of the primary transmitter against the transmitter info of the TAVs (if it is available), and all the TAVs which are set by the primary transmitter are reset. This ensures that the TAV of the secondary transmitter is not set by either the RTS or the PTS sent by the primary transmitter. If it finds the medium to be free and has a suitable packet to be transmitted, it responds with a Clear to Transmit (CTT) frame whose format is the same as the CTS (Fig. 10). Transmission of the CTT implies that the secondary transmitter is capable of transmitting overlapped data without causing interference to any of the transmissions (including the primary transmission) in its communication range.

In the example network of Fig. 8(a), when B receives the PTS from C, it ensures that its TAV is set only by C's transmission of RTS to D (refer to the TAV0 setting of B shown in Fig. 9). Since B is not in the transmission range of D, it will be able to detect D's transmission of CTS but will not be able to decode it. This would cause B's TAV1 to be set to a duration of Extended Inter Frame Spacing (EIFS) [21] but it would expire before the PTS frame is received (refer to TAV1 setting of B in Fig. 9). Based on the selection criteria for choosing a partner, assume node B chooses node A to send the RTT. When A receives the RTT, it ensures that its TAV vector is not set (refer to the TAV settings of A in Fig. 9). If it senses the medium to be free, it responds with a CTT frame. In the present example, if we assume that A is in the interference range of C (it can sense C's transmission but not decode it), it would have set its TAV (when C transmits PTS to B) to EIFS which would have expired by the time A receives the RTT frame.

C. Primary transmission

A timer at the primary transmitter is set to expire in synchronous with the completion of the secondary handshaking. Note that its TAV timer will not be set during the transmission of the secondary handshaking (refer to the TAV settings of node C in Fig. 9). We note that this differs from the typical NAV vector implementation of IEEE 802.11 protocol. When the timer expires, it commences the transmission of the data frame to the primary receiver. This is shown in Fig. 8(g).

[2]Using other approaches such as round robin scheduling, may increase the probability of choosing a node with a packet for the secondary receiver.

D. Secondary transmission

After the transmission of the CTT frame, the secondary transmitter starts a timer such that it expires Δ_0 seconds after the commencement of the primary transmission. This *overlapped delay* Δ_0 is a design parameter which results in a delayed transmission of the secondary transmission. This delay between the primary and secondary transmissions is intended for the secondary receiver to acquire the signal from the primary transmitter. The value of this overlapped delay is chosen based on the physical layer (PHY) parameters such as the Physical Layer Convergence Protocol (PLCP) header length such that the signal from the primary transmitter can be acquired by the secondary receiver. Note that the design of this delayed transmission of the overlapped data doesn't ensure perfect synchronization of both the primary and secondary transmissions at the secondary receiver. However, this delay ensures that the secondary receiver acquires the signal of the primary transmitter which greatly simplifies the interference cancellation (IC) mechanism at the PHY layer. The format of the overlapped data (O-DATA) frame is same as the data frame. The secondary receiver cancels out the interference and recovers the overlapped data. This phase is illustrated in Fig. 8(h). Note that the secondary transmission is allowed to terminate Δ_1 seconds after the end of the primary transmission.

E. Data Acknowledgments

After the DATA and O-DATA are successfully received, the primary and secondary transmitters acknowledge the successful reception of the primary and overlapped data frames as shown in Figs. 8(i) and 8(j), respectively.

First, consider the successful reception of the DATA and O-DATA frames at the primary and secondary receivers. These nodes contend for the channel access if they have packets to transmit. The channel access mechanism for the primary receiver is the same as the mechanism in the IEEE 802.11 protocol [21]. However, the channel access mechanism for the secondary receiver is slightly different. If the secondary receiver is forwarding the current O-DATA frame, and finds the medium to be free, it starts its backoff timer with the contention window (CW) size twice the current CW value (at the secondary receiver). This ensures that, with high probability, the secondary receiver is in backoff for a greater duration than the primary receiver. Hence, the secondary receiver will not contend with the primary receiver for channel access.

Next, consider the reception of acknowledgments at the primary and secondary transmitters. Upon reception of ACK, the primary transmitter resets it contention window (CW) parameter as in the IEEE 802.11 [21] protocol. If it has a packet to transmit, the channel access mechanism is same as the mechanism in the IEEE 802.11 protocol. However, the secondary transmitter does not reset its CW. This ensures that, with high probability, the secondary transmitter does not contend with the primary transmitter for channel access. The CW parameter of the secondary transmitter is reset when it receives an ACK for any DATA frame that it transmits later. We observed that, in networks with linear flows, this design leads to a greater probability of overlapped transmission.

V. Design Considerations

In this section, we discuss various design issues concerning the OCSMA protocol. In particular, we compare and contrast the OCSMA protocol with the IEEE 802.11 MAC protocol, on which it is based.

A. Cross-layer interaction

The design of OCSMA protocol involves a greater level of cross-layer interaction compared to the IEEE 802.11 protocol. For instance, when a node receives an RTT, the MAC needs to interact with the higher layers to determine if a packet of suitable length can be sent to the secondary receiver. It is also possible that a packet might need fragmentation such that the transmission of overlapped data is terminated within Δ_1 seconds of the termination of the primary transmission (refer to the timeline of the protocol in 9). Similarly, when the secondary receiver receives a CTT, the MAC needs to indicate the PHY layer regarding the arrival of overlapped data so that the interference mitigation mechanism can be activated. Cross-layer interaction is also needed at the secondary transmitter when identifying potential partners for overlapped transmission.

B. Complexity of the protocol

The OCSMA protocol involves greater computational complexity than the IEEE 802.11 protocol. This is a result of employing MUD at the PHY and also increased bookkeeping in the MAC. However, the increase in the computational complexity at the MAC is minimal, and we believe that the design of the protocol can greatly reduce the computational complexity at the PHY layer in comparison to the other MUD approaches. We also note that the protocol overhead of OCSMA is more than that of IEEE 802.11 due to an increase in the number of control frames. However, as the results in Section VI indicate, this overhead becomes negligible as the size of the data frame increases.

C. Reduced Overhead

The design of protocol and the frame formats are compatible with the existing 802.11 frame formats to a large extent. Hence they can be integrated with the existing wireless networks with minimal changes. The overhead of the OCSMA protocol can be reduced considerably if no such conformity is required. For instance the CTT packet can be eliminated without a significant penalty on the throughput. The elimination of CTT packet results in reduced protocol overhead but increases the power consumption at PHY of the secondary receiver since the interference cancelation has to be turned on more often. In addition, the DA fields of the PTS and RTT frames can be eliminated without any significant performance penalty (refer to Fig. 10). We call this protocol the OCSMA protocol with reduced overhead (OCSMA_RO). The performance of this reduced overhead protocol is simulated in the next section. The PTS can be also be eliminated by including the information of PTS frame in the RTS. In this case, the RTS format will be much different from the format of RTS of the 802.11 protocol. However, we did not observe any significant change in the throughput with this modification. Finally, the frame formats of all the frames can be modified to reduce the overhead, although we did not evaluate such approaches in this article.

VI. Simulation Results

In this section, we evaluate the performance of the OCSMA protocol under different network topologies and traffic conditions using Network Simulator (ns2) [22]. Since we evaluate only the performance of the MAC protocol, we assume perfect interference cancelation at the PHY layer, and that the O-DATA packet can be recovered whenever there is an overlapped transmission with the corresponding primary transmission being the only source of interference. The simulation parameters used for all the simulations in this section are given in Table I. Unless specified otherwise, the default values of these parameters are used in the simulations. The overlapped delay Δ_0 is chosen to be equal to 240 μs, which corresponds to about 30 bytes of data transmitted at a rate of 1 Mbps. The data length of 30 bytes is slightly greater than the PCLP header length of 24 bytes. The value of Δ_1 is chosen to be equal to Δ_0. For other system parameters, the default values of the 802.11 implementation of ns2 are used.

TABLE I
Simulation setup.

Parameter	Default value
Bandwidth	1 MHz
Data rate	1 Mbps
Simulation duration	4000 s
Warmup time	400 s
Routing protocol	AODV
Channel model	Two ray propagation
RTS Threshold	150 Bytes
Transmission radius	250 m
Carrier-sensing radius	550 m
IFQ length	100
Overlapped Delay Δ_0	240 μs
Δ_1	240 μs
STA Short Retry Limit	7
STA Long Retry Limit	4

We first evaluate the OCSMA protocol under fixed network topologies. The network under consideration is a ten-node linear network, with the source and destination located at either end of the network. The nodes are placed at regular intervals with adjacent nodes being in the communication range of each other, and nodes two hops apart being in the interference range of each other. The transmission power of the secondary transmission is the same as that of the primary transmission. The traffic type is TCP with a maximum window size of 32. The end-to-end throughputs of the network under the OCSMA, OCSMA_RO, and IEEE 802.11 MAC protocols are shown in Fig. 11.

We observe that the throughput of IEEE 802.11 MAC protocol increases until data packet length of 1000 bytes, beyond which it starts decreasing. However, the throughput of both OCSMA and OCSMA_RO increase until the packet length reaches 1400 bytes, beyond which the throughput decreases. The OCSMA protocol provides throughput gains of 4-39% over the range of packet lengths shown in Fig. 11. The maximum throughput under OCSMA is achieved for a packet length of 1400 bytes, at which point it provides 21% throughput gain over IEEE 802.11. Similarly, the reduced overhead version of OCSMA (OCSMA_RO) provides throughput gains of 11-40% over the packet lengths simulated, and provides a throughput gain of 28% over 802.11 for a packet length of 1400 bytes.

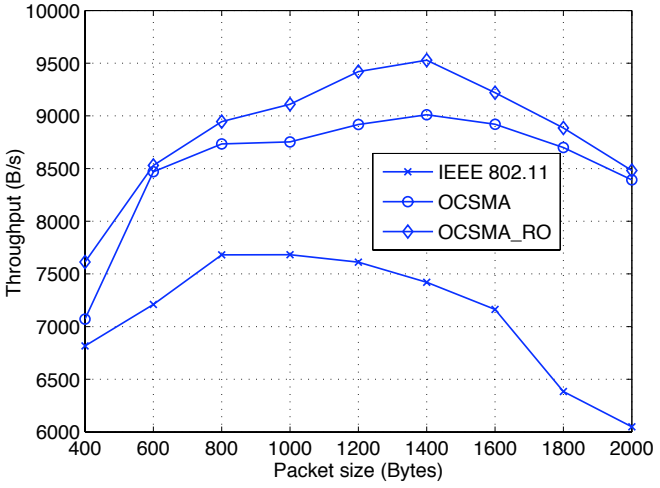

Fig. 11. Throughput comparison in a ten-node linear network with TCP traffic.

The MAC level events across the network of all three protocols are tabulated in Table II and Table III for data packet lengths 400 and 1800 bytes, respectively. It can be seen that the average rate of RTS frames received at the MAC level of all the nodes in the case of OCSMA and OCSMA_RO is higher than the rate of RTS frames received in the case of IEEE 802.11. We observe that the proportion of the average rate of reception of PTS to that of RTS is very high indicating that there is a very high probability of an overlapped transmission from the perspective of the primary transmitter. However, the ratio of the reception of CTT to that of RTT is significantly lower, which indicates that the actual number of overlapped data transmissions are significantly less than the potential overlapped transmissions. This might be due to the lack of suitable packets at the secondary transmitter, or the medium being busy as perceived by the secondary transmitter. In order to investigate the reason for a very low ratio of CTT to RTT frames in the network, we created a No Packet to Transmit (NPT) frame. The NPT frame is transmitted by a secondary receiver in response to an RTT if it finds the medium to be free but doesn't have a suitable packet for the secondary receiver. The NPT frame was introduced only for simulation purposes, and is not a part of the OCSMA protocol. We did not observe any adverse effect on the system throughput of this ten-node linear network due to the inclusion of the NPT frame.

As can be seen in Table II and Table III , the ratio of CTT to NPT is about 54%, and 41% for packet lengths 400 bytes and 1800 bytes, respectively. This indicates that the full potential of the overlapped transmissions is not realized due to lack of suitable packets. The ratio of overlapped data (O-DATA) packets received to that of data (DATA) packets is 19.5% and 17.9% for OCSMA and OCSMA_RO, respectively, for a packet size of 400 bytes. The ratio is 17.9% and 17.3%, respectively, when the packet size is increased to 1800 bytes. It is also worth noting that the average number of collisions at the MAC level in the case of both the OCSMA protocols is higher than that of IEEE 802.11 protocol. We observed that these collisions are mainly due to the control frames during the secondary handshaking (RTT and CTT) causing collisions in the vicinity of the secondary transmitter. However, these collisions are offset by the increase in throughput due to

overlapped transmissions.

TABLE II
COMPARISON OF EVENTS AT THE MAC LEVEL FOR A TEN NODE LINEAR NETWORK WITH PACKET SIZE 400B .

Received packet type	IEEE 802.11 (Events/s)	OCSMA (Events/s)	OCSMA_RO (Events/s)
RTS	161.8	193.6	201.0
CTS	136.2	127.9	140.0
PTS	-	110.8	105.8
RTT	-	79.1	78.9
CTT	-	22.8	-
NPT	-	41.8	-
DATA	134.0	117.0	127
O-DATA	-	22.8	22.7
Collision	9.3	15.5	10.1

TABLE III
COMPARISON OF EVENTS AT THE MAC LEVEL FOR A TEN NODE NETWORK WITH PACKET SIZE 1800B.

Received packet type	IEEE 802.11 (Events/s)	OCSMA (Events/s)	OCSMA_RO (Events/s)
RTS	36.0	59.5	61.0
CTS	32.4	39.5	41.5
PTS	-	34.4	36.0
RTT	-	26.0	28.0
CTT	-	6.7	-
NPT	-	16.4	-
DATA	32.3	39.0	41
O-DATA	-	6.7	7.1
Collision	0.7	3.2	3.2

Next, we evaluate the impact of TCP window size on the throughput of OCSMA and OCSMA_RO protocols. The throughput gains of OCSMA and OCSMA_RO protocols over IEEE 802.11 as a function of the TCP window size is shown in Fig. 12. The throughput of OCSMA protocols is less than that of the IEE 802.11 for TCP window sizes 2 and 4. This is due to the unavailability of packets at the secondary transmitters to perform overlapped transmissions. As the TCP window size increases, the throughput gains of both OCSMA and OCSMA_RO increase, providing a maximum gain of 21% and 30%, respectively, for window sizes greater than 16.

The MAC level events for the OCSMA protocol for several window sizes are shown in Table IV. It can be seen that the ratio of the CTT to NPT frames increases with an increase in the TCP window size. We also observe that the collision rate increases as the TCP window size increases. Since the collision rate for OCSMA protocols is higher than that of IEEE 802.11, we next analyze the impact of the STA Short Retry Count (ssrc), and STA Long Retry Count (slrc) limits on the throughput of OCSMA and OCSMA_RO. Fig. 13 shows the throughput gains of OCSMA and OCSMA_RO over IEEE 802.11 for various values of ssrc and slrc limits. The TCP window size is 32 and the packet size is 1400 bytes. The values of the slrc and ssrc limits used are shown in parenthesis. We observe that the throughput gain of OCSMA and OCSMA_RO increase monotonically with an increase in ssrc and slrc limits. The increase in the collisions in the case of OCSMA protocols are offset by the increase in the ssrc and slrc limits.

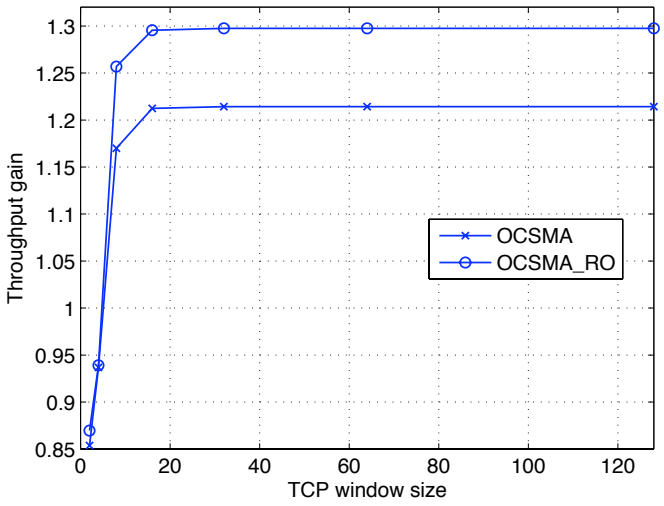

Fig. 12. Throughput gains of OCSMA and OCSMA_RO in a ten-node linear network.

TABLE IV
EVENTS AT THE MAC LEVEL IN THE OCSMA PROTOCOL.

Received packet type	CW = 2 (Events/s)	CW = 8 (Events/s)	CW = 64 (Events/s)
RTS	86.5	75.6	79.4
CTS	73.5	49.9	52.0
PTS	65.0	43.3	46.1
RTT	53.2	32.3	33.7
CTT	11.0	8.4	8.8
NPT	39.8	19.7	20.0
DATA	71.1	46	48.0
O-DATA	11.0	8.4	8.8
Collision	2.4	4.0	4.2

The throughputs of a ten-node linear network under IEEE 802.11, OCSMA and OCSMA_RO protocols with constant bit rate (CBR) traffic is shown in Fig. 14 for several packet arrival rates. The packet size is 1000 bytes. We observe that the throughput of all the three protocols is the same until the packet arrival rate reaches 20 packets/s. As the packet rate increases, there is a dramatic fall in the rate of packets delivered in the case of IEEE 802.11. However, under OCSMA and OCSMA_RO, the decline in the throughput is more gradual, and the throughput gains provided by OCSMA protocols over IEEE 802.11 is significant.

Next, we consider the effect of multiple-flows in a linear network. Three sources and three destinations are placed at either end of a ten-node linear network, and the traffic type is CBR. The throughput gains of OCSMA and OCSMA_RO over 802.11 with CBR traffic and multiples flows in a linear network is shown in Fig. 15. The packet arrival rate indicates the common rate at which packets arrive at each of the sources. It can be observed that even in the presence of multiple flows, OCSMA and OCSMA_RO provide significant gains over IEEE 802.11 in a ten-node linear network. The next scenario we consider is a linear network topology with variable number of nodes. The network has a single source and a single destination located at opposite ends of the network. TCP traffic with a packet size of 1400 bytes was simulated. The other simulation parameters

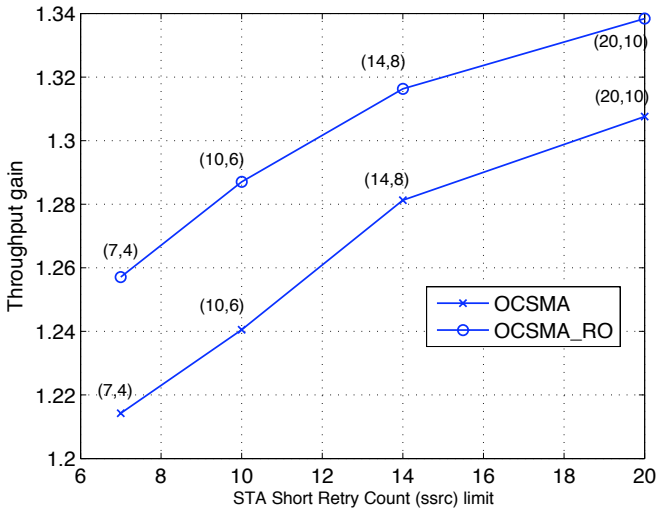

Fig. 13. Throughput gains of OCSMA and OCSMA_RO in a ten-node linear network.

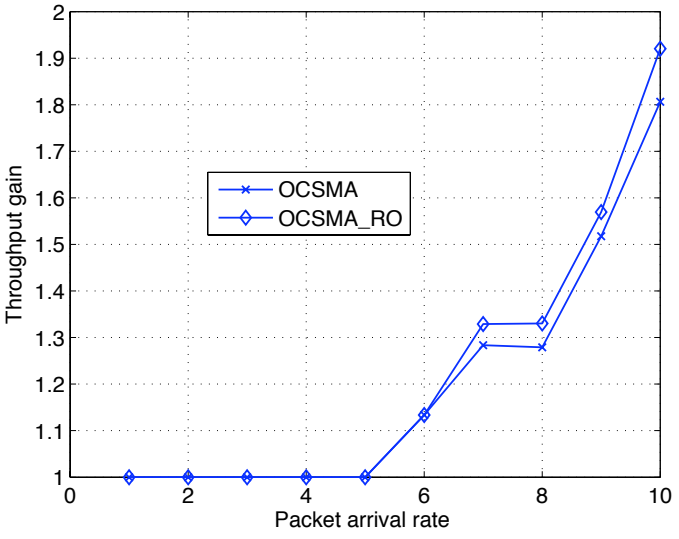

Fig. 15. Throughput comparison in linear network with multiple flows.

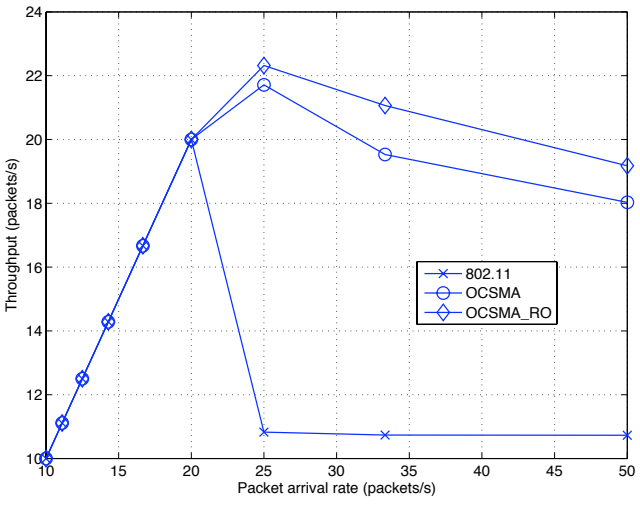

Fig. 14. Throughput comparison in a ten-node linear network with CBR traffic.

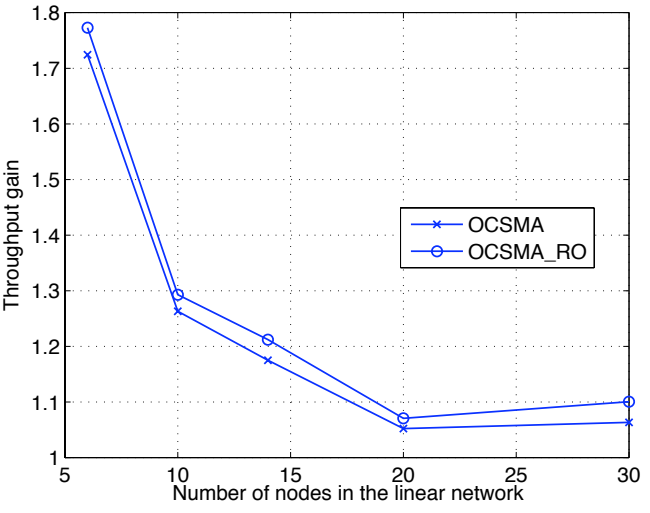

Fig. 16. Throughput gain of OCSMA and OCSMA_RO in a linear network.

are given in Table I. The end-to-end throughput gains of the OCSMA and OCSMA_RO protocols over IEEE 802.11 are shown in Fig. 16 as a function of the number of nodes in the linear network. It can be seen that OCSMA and OCSMA_RO provide maximum throughput gains of 72% and 77%, respectively, when the network consists of six nodes. The gain decreases with an increase in the number of nodes in the network. In a thirty-node network, the throughput gains of OCSMA and OCSMA_RO are 16% and 10%, respectively. For a fixed TCP window size, under OCSMA and OCSMA_RO, we observed that, as the size of the linear network increases, the ratio of O-DATA to DATA frames decreases and the collision rate increases. The increase in the spatial re-use provided by OCSMA (and OCSMA_RO) is offset by the increase in the collisions in the network.

We also evaluated the throughput gains of OCSMA and OCSMA_RO over 802.11 in a binary tree network. In this topology, each node of the tree network has exactly two children, and the root transmits independent messages to each of the leaf nodes. The traffic type is CBR, and the packets meant for each of the leaf nodes arrive at the source with same rate. The performance gains of OCSMA and OCSMA_RO in a binary tree network with a depth of four is shown in Fig. 17. It can be observed that for packet arrival rates greater than 3, OCSMA and OCSMA_RO provide at least 35% throughput gain over IEEE 802.11 protocol.

The next network topology we consider is a random topology with 50 nodes randomly distributed in a square of dimension 1500m X 1500m. This scenario corresponds to a node density of four nodes in a circle of radius equal to the transmission range of a node (set to 250m). The mobility model chosen is the random way point model, which is the default model in ns2. The nodes move with a speed that is uniformly distributed in the interval $[0, \text{max\_speed}]$, where we consider different values of max_speed. Twenty TCP connections were randomly generated with packet

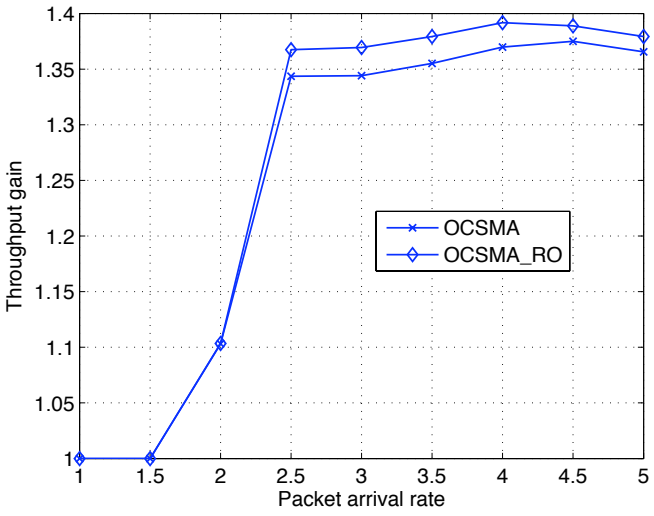

Fig. 17. Throughput gain of OCSMA and OCSMA_RO in a tree network.

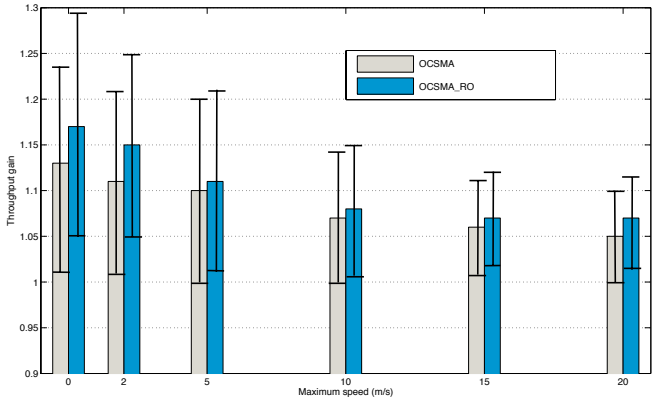

Fig. 18. Throughput gain in a random network with mobility.

size 1400 bytes, and the rest of the system parameters are given in Table I. The throughput gains of OCSMA and OCSMA_RO over IEEE 802.11 are averaged over 500 instantiations of the random network. The performance gain of OCSMA protocols over IEEE 802.11 as a function of the maximum speed of the nodes in the network is shown Fig. 18. We observe that the throughput gain of the OCSMA protocols decrease as the mobility in the network increases. When there is no mobility in the network, OCSMA provides and average throughput gain of about 13% with a standard deviation of 0.11. The high standard deviation indicates that in certain scenarios, OCSMA provides significant gains over 802.11 protocol. Similarly, OCSMA_RO provides an average throughput gain of 17% with a standard deviation of 0.12. When there is high mobility in the network (max_speed = 20m/s), OCSMA provides an average gain of 5% (standard deviation = 0.05), and OCSMA_RO provides an average gain of 7% (standard deviation = 0.05). The results indicate that, in general, the throughput gain from overlapped transmissions is not significant when there is high mobility in the network. However, in certain scenarios, OCSMA provides significant gain over IEEE 802.11 protocol.

We also observed that, in certain scenarios, the performance of the OCSMA protocol is much worse than that of the 802.11 protocol. In these scenarios, the increase in the spatial re-use due to overlapped transmissions increased the number of inter-flow contentions, which affected the throughput of the network. We are currently investigating the inter-flow contention issues associated with the OCSMA protocol.

VII. Conclusion

In this work, we studied the use of overlapped transmission to enhance the spatial re-use and throughput of wireless networks. By taking advantage of *a priori* knowledge of the interfering packet, the receiver can employ a simplified IC scheme to receive a packet in the presence of interference. We analyzed some of the factors that limit the use of overlapped transmissions in an ad hoc network.

We developed the OCSMA protocol based on the IEEE 802.11 MAC protocol to support overlapped transmissions in a wireless network. OCSMA has greater MAC overhead and increased computational complexity at the PHY layer, but the increase in the spatial re-use of the network and throughput gain may justify these in many scenarios. Network simulations employing OCSMA protocol and its reduced overhead variant, OCSMA_RO, show that the end-to-end throughput can be improved by as much as 77% over IEEE 802.11 protocol in a linear network with TCP traffic. Under CBR traffic, OCSMA and OCSMA_RO are more robust to the traffic load and multiple flows than the IEEE 802.11 protocol. In a random network with 50 nodes and 20 TCP connections, the OCSMA and OCSMA_RO protocols provide an average throughput gain of 13% and 17%, respectively, when there is no mobility in the network. The throughput gain of the OCSMA protocols decrease with an increase in the mobility in the network. Although the average gain provided by the OCSMA protocols in high mobility conditions is only 5% to 7%, the throughput gain in certain scenarios can be much higher.

Appendix I
Derivation of the joint pdf of X_{AD}, X_{CD}

In order to evaluate the joint distribution of X_{AD} and X_{CD}, we first look at the relative positions of nodes A and D with respect to node B. Note that A is uniformly distributed in an unit circle with B at the centre. The density function of X_{AB}, the distance between A and B is given by

$$f_{X_{AB}}(x) = \begin{cases} 2x, & 0 \le x \le 1 \\ 0, & \text{otherwise.} \end{cases} \tag{16}$$

Similarly, node C is also uniformly distributed within the transmission range of B, and hence the pdf of X_{BC} is the same as that of X_{AB}. Node D is in the transmission range of C but not in the transmission range of B. Hence, it is uniformly distributed in the shaded region of Fig. 3. The joint conditional distribution of X_{CD} and X_{BD} given X_{BC} can be derived in a similar fashion and is given by (refer to Fig. 19)

$$F_{X_{CD},X_{BD}}(y,z|X_{BC}=x) = \begin{cases} \frac{\pi y^2 - \mathcal{A}_l(1,y,x)}{\pi - \mathcal{A}_l(1,1,x)}, & z > x+y \\ \frac{\mathcal{A}_l(z,y,x) - \mathcal{A}_l(1,y,x)}{\pi - \mathcal{A}_l(1,1,x)}, & z < x+y, \end{cases} \tag{17}$$

$$f_{X_{CD}X_{BD}}(y,z|X_{BC}=x)=\begin{cases}\frac{1}{\pi-\mathcal{A}_l(1,1,x)}\frac{4yz}{\sqrt{(x+y+z)(x+y-z)(x-y+z)(-x+y+z)}}, & 0\le x,y\le 1,\\ & 1<z\le x+y,\\ 0, & \text{otherwise.}\end{cases} \tag{18}$$

$$f_{X_{AD}X_{CD}}(s,y)=\int_x\int_z f_{X_{AD}}(s|x,y,z)f_{X_{CD},X_{BD}}(y,z|x)f_{BC}(x)dzdx. \tag{19}$$

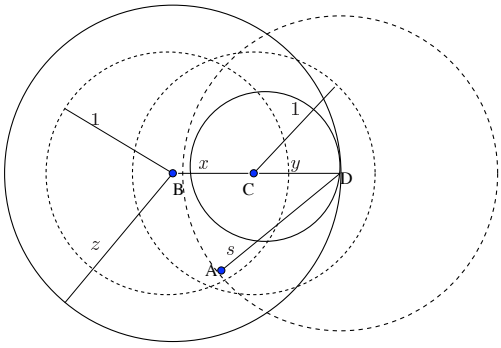

Fig. 19. Circle-circle intersection for analysis.

where $\mathcal{A}_l(1,y,x)$ is given by (4). The conditional joint density function is given (18). Since A is uniformly distributed in a unit circle with B at the center, the conditional distribution of X_{AD}, the distance between nodes A and D is given by

$$F_{X_{AD}}(s|X_{BD}=z)=\begin{cases}\frac{1}{\pi}\mathcal{A}_l(1,s,z), & s+1>z,\\ 0, & \text{otherwise.}\end{cases} \tag{20}$$

and the pdf is given by

$$f_{X_{AD}}(s|X_{BD}=z)=\begin{cases}\frac{2s}{\pi}\cos^{-1}\left(\frac{s^2+z^2-1}{2sz}\right), & s+1>z,\\ 0, & \text{otherwise.}\end{cases} \tag{21}$$

Note that X_{AD} is conditionally independent of X_{CD}, X_{BC} given X_{BD}. Hence

$$f_{X_{AD}}(s|X_{CD}=x,X_{BC}=y,X_{BD}=z)=f_{X_{AD}}(s|X_{BD}=z). \tag{22}$$

The joint distribution of X_{AD} and X_{CD} is given by (19).

REFERENCES

[1] S. Ghez, S. Verdu, and S. C. Schwartz, "Stability properties of slotted Aloha with multipacket reception capability," *Automatic Control, IEEE Transactions on*, vol. 33, pp. 640–649, July 1988.

[2] J. Q. Bao and L. Tong, "Performance analysis of slotted Aloha random access ad-hoc networks with multipacket reception," in *Military Communications Conference Proceedings, 1999. MILCOM 1999. IEEE*, Nov. 1999, vol. 1, pp. 251–255.

[3] Q. Zhao and L. Tong, "Semi-blind collision resolution in random access wireless ad hoc networks," *Signal Processing, IEEE Transactions on*, vol. 48, pp. 2910–2920, Oct. 2000.

[4] M. Howlader, K. Mostofa, and B. D. Woerner, "System architecture for implementing multiuser detector within an ad-hoc network," in *Military Communications Conference, 2001. MILCOM 2001. Communications for Network-Centric Operations: Creating the Information Force. IEEE*, Oct. 2001, vol. 2, pp. 1119–1123.

[5] R. M. de Moraes, R. Sadjadpour, and J. J. Garcia-Luna-Aceves, "A new communication scheme for MANETs," in *Wireless Networks, Communications and Mobile Computing, 2005 International Conference on*, June 2005, vol. 2, pp. 1331–1336.

[6] C. Comaniciu, N. B. Mandayam, and H. V. Poor, *Wireless Networks: Multiuser Detection in Cross-layer Design*, Springer, 2005.

[7] V. Naware, G. Mergen, and L. Tong, "Stability and delay of finite-user slotted ALOHA with multipacket reception," *Information Theory, IEEE Transactions on*, vol. 51, no. 7, pp. 2636–2656, July 2005.

[8] G. Mergen and L. Tong, "Receiver controlled medium access in multihop ad hoc networks with multipacket reception," in *Military Communications Conference, 2001. MILCOM 2001. Communications for Network-Centric Operations: Creating the Information Force.*, Oct. 2001, vol. 2, pp. 1014–1018.

[9] S. Boppana and J. M. Shea, "Overlapped transmission in wireless ad hoc networks," in *Proc. 2006 Int. Conf. Commun. Circuits and Systems*, Guilin, China, Jun. 2006, vol. 2, pp. 1309–1314.

[10] D.S. Lun, M. Medard, R. Koetter, and M. Effros, "On Coding for Reliable Communication over Packet Networks," *Arxiv preprint cs.IT/0510070*, 2005.

[11] S. Chachulski, M. Jennings, S. Katti, and D. Katabi, "Trading structure for randomness in wireless opportunistic routing," *SIGCOMM Comput. Commun. Rev.*, vol. 37, no. 4, pp. 169–180, 2007.

[12] C. Fragouli and E. Soljanin, "Information flow decomposition for network coding," *Information Theory, IEEE Transactions on*, vol. 52, no. 3, pp. 829–848, Mar. 2006.

[13] Y. E. Sagduyu and A. Ephremides, "Crosslayer design for distributed MAC and network coding in wireless ad hoc networks," *Information Theory, 2005. ISIT 2005. Proceedings. International Symposium on*, pp. 1863–1867, Sep. 2005.

[14] E. Fasolo, M. Rossi, J. Widmer, and M. Zorzi, "On MAC Scheduling and Packet Combination Strategies for Practical Random Network Coding," *Communications, 2007. ICC'07. IEEE International Conference on*, pp. 3582–3589, Jun. 2007.

[15] S. Katti, H. Rahul, W. Hu, D. Katabi, M. Médard, and J. Crowcroft, "XORs in the air: practical wireless network coding," *SIGCOMM '06: Proceedings of the 2006 conference on Applications, technologies, architectures, and protocols for computer communications*, pp. 243–254, 2006.

[16] R. Koetter, "Network coding bibliography," *URL: http://tesla. csl. uiuc. edu/~ koetter/NWC/Bibliography. html*.

[17] S. Zhang, S. C. Liew, and P. Lam, "Physical-layer network coding," in *The Annual International Conference on Mobile Computing and Networking*, Los Angeles, Sep. 2006, pp. 358–365.

[18] J. Zhang, K. Cai, K. B. Letaief, and P. Fan, "A network coding unicast strategy for wireless multi-hop networks," in *Wireless Communications and Networking Conference, 2007.WCNC 2007. IEEE*, Hong Kong, Mar. 2007, pp. 4221–4226.

[19] S. Katti, S. Gollakota, and D. Katabi, "Embracing wireless interference: analog network coding," in *SIGCOMM '07: Proceedings of the 2007 conference on Applications, technologies, architectures, and protocols for computer communications*. 2007, pp. 397–408, ACM Press New York, NY, USA.

[20] Y. Hao, D. Goeckel, Z. Ding, D. Towsley, and K.K. Leung, "Achievable Rates of Physical Layer Network Coding Schemes on the Exchange Channel," *Military Communications Conference Proceedings, 2007. MILCOM 2007. IEEE*, Oct. 2007.

[21] IEEE 802.11 WLAN Committee, "IEEE P802.11, the working group setting standards for wireless LANs," Web page: `http://grouper.ieee.org/groups/802/11/`, Current as of May 30, 2007.

[22] K. Fall, K. Varadhan, et al., "The ns-2 manual," *the VINT Project, http://www.isi.edu/nsnam/ns/doc/*, 2007.